Original Article

DOI: 10.5582/bst.2024.01249

FNDC5/Irisin mitigates high glucose-induced neurotoxicity in HT22 cell *via* ferroptosis

Lingling Yang[1,§], Xiaohan Zhou[1,§], Tian Heng[1], Yinghai Zhu[1,2], Lihuan Gong[1], Na Liu[1], Xiuqing Yao[1,3,4,*], Yaxi Luo[1,*]

[1] Department of Rehabilitation, The Second Affiliated Hospital of Chongqing Medical University, Chongqing, China;
[2] Department of Rehabilitation, The Central Hospital of Enshi Tujia and Miao Autonomous Prefecture, Enshi Clinical College of Wuhan University, Enshi, China;
[3] Chongqing Municipality Clinical Research Center for Geriatric Medicine, Chongqing, China;
[4] Department of Rehabilitation Therapy, Chongqing Medical University, Chongqing, China.

SUMMARY Diabetes-induced neuropathy represents a major etiology of dementia, highlighting an urgent need for the development of effective therapeutic interventions. In this study, we explored the role of fibronectin type III domain containing 5 (FNDC5)/Irisin in mitigating hyperglycemia-induced neurotoxicity in HT22 cells and investigated the underlying mechanisms. Our findings reveal that high glucose conditions are neurotoxic, leading to reduced viability of HT22 cells and increased apoptosis. Furthermore, the elevated expression of the intracellular ferroptosis marker Acyl-CoA Synthetase Long Chain Family Member 4 (ACSL4), along with increased levels of ferrous ions and malondialdehyde (MDA), suggests that high glucose conditions may induce ferroptosis in HT22 cells. FNDC5/Irisin treatment effectively mitigates high glucose-induced neurotoxicity and ferroptosis in HT22 cells. Mechanistically, FNDC5/Irisin enhances cellular antioxidant capacity, regulates ACSL4 expression, and improves intracellular redox status, thereby inhibiting ferroptosis and increasing HT22 cell survival under high-glucose conditions. These results highlight the neuroprotective potential of FNDC5/Irisin in high glucose environments, offering a promising avenue for developing treatments for diabetes-related neurodegenerative diseases.

Keywords high-glucose environment, neurotoxicity, FNDC5/Irisin, ferroptosis

1. Introduction

Type 2 diabetes mellitus (T2DM) comprises approximately 96% of all diabetes cases (*1-4*). Notably, the prevalence of mild cognitive impairment among individuals with T2DM reaches as high as 45% (*5*), a major contributor to dementia and a potentially modifiable risk factor (*6*). As such, diabetes-induced brain aging and cognitive decline are significant complications, underscoring the importance of investigating the mechanisms underlying hyperglycemia-driven cognitive dysfunction for the prevention and amelioration of diabetic brain injury.

Studies have identified ferroptosis as a key driver of diabetic cognitive dysfunction, with increased iron deposition observed in the brains of patients with T2DM and cognitive impairment (*7*). Excess iron catalyzes the Fenton reaction, resulting in the overproduction of reactive oxygen species (ROS), which subsequently depletes glutathione, triggers lipid peroxidation, and exhausts endogenous antioxidant defenses, ultimately leading to neuronal ferroptosis, synaptic dysfunction, and cognitive decline (*8*). Inhibition of ferroptosis has been shown to mitigate hippocampal neuronal damage and synaptic plasticity impairments, effectively improving cognitive function (*9-11*). These findings suggest that high-glucose-induced neurotoxicity is closely associated with ferroptosis, highlighting the inhibition of ferroptosis as a promising therapeutic strategy for alleviating cognitive deficits in T2DM.

The FNDC5 gene is highly expressed in the hippocampus and cortex of C57BL/6 mice (*12*). Its cleaved form, irisin, has been detected in the cerebrospinal fluid (*13,14*). Studies suggest that FNDC5/irisin plays a critical role in cognitive and memory functions (*14,15*). Furthermore, FNDC5/irisin attenuates high-glucose-induced cytotoxicity via the AMPK-insulin receptor signaling pathway (*16-18*). In addition, irisin has been implicated in ferroptosis regulation in a mouse model of sepsis-associated encephalopathy, where

FNDC5/irisin reduced $Fe2^{+}$, ROS, malondialdehyde (MDA), and acyl-CoA synthetase long-chain family member 4 (ACSL4) levels, thereby inhibiting ferroptosis and improving learning and memory functions (*19*). However, whether FNDC5/irisin can mitigate high-glucose-induced neurotoxicity by inhibiting ferroptosis remains unclear and warrants further investigation.

In this study, we observed that high glucose conditions induced neurotoxicity and triggered ferroptosis in HT22 cells. Irisin treatment effectively mitigated high glucose-induced neurotoxicity and ferroptosis. Additionally, we found that high glucose reduced the expression of FNDC5 in HT22 cells. Overexpression of FNDC5 attenuated high glucose-induced neurotoxicity, enhanced synaptic plasticity, and inhibited ferroptosis. Exogenous irisin supplementation also effectively alleviated hyperglycemic neurotoxicity and ferroptosis in the context of reduced FNDC5 expression. In summary, our data suggest that FNDC5/irisin exerts neuroprotective effects through the inhibition of ferroptosis under high glucose conditions, providing new insights into diabetes-induced cognitive impairment.

2. Materials and Methods

2.1. Cell culture and glucose treatment

HT22 murine hippocampal cells was kindly provided by the Chongqing Key Laboratory of Translational Medicine for Cognitive Development and Learning and Memory Disorders, Institute of Pediatrics, Children's Hospital of Chongqing Medical University. The cells were cultured in Dulbecco's modified Eagle's medium supplemented with 10% fetal bovine serum, 100 U/mL penicillin and 100 μg/mL streptomycin. For high glucose treatment, 750 mM stock solution of high glucose was prepared with D-(+)-glucose and glucose-free medium and diluted to different concentrations with glucose-free complete medium. 25 μg of Irisin lyophilized powder was added with 250 μL of glucose-free medium and mixed slowly up and down to make a stock solution of Irisin at a concentration of 100 ng/mL, and then diluted to gradient dilution with the corresponding glucose-concentrated medium according to the need of the experiments. All cells were cultured in a humidified cell culture incubator (Thermo Fisher) at 37°C with 5% CO_2.

2.2. Cell transfection

Plasmid transfection sequences were designed by Shanghai Genechem Co., For gene overexpression, the FNDC5 overexpression plasmid (CMV enhancer-MCS-3flag-polyA-EF1A-zsGreen-sv40-puromycin) was constructed by cloning the corresponding coding sequence into the GV657 vector. For knockdown, the FNDC5 knockdown plasmid (hU6-MCS-CBh-gcGFP-IRES-puromycin) was constructed by cloning the corresponding coding sequence into the GV493 vector. lipofectamine 3000 reagent (Invitrogen, cat # L3000015, USA) was used for cell transfection according to the manufacturer's instructions. 48 hours after transfection, cells were used for further experiments.

2.3. Chemicals

Irisin(# 8880) purchased from R&D, fetal bovine serum(#10099141C), penicillin-streptomycin(#15140122), 0.25%Trypsin-EDTA(1×) (#25200056), basic DMEM (#C11995500BT), DMEM, glucose free (#11966025) , Opti-MEM™ I serum reduced media (#31985062) purchased from Gibco, bovine serum albumin (#A8020), D-(+)-glucose(#G6152), D-Mannitol(#M4125), ferroptosis inhibitor ferrostatin-1 (fer-1) (#SML0583) purchased from sigma, ferroptosis inducer Erastin (#HY-15763) purchased from MCE.

2.4. CCK-8 assay

The CCK-8 (MCE, #HY-K0301, USA) assay kit was used to assess cell viability precisely according to the instructions. HT22 cells were intervened as required for the experiment, and the medium was replaced with CCK-8 working solution containing 10% CCK-8 reagent after treatment. Cells were incubated at 37°C for 1 hour. A microplate reader measured the absorbance (450 nm) of each well.

2.5. FerroOrange staining

Intracellular Fe^{2+} was detected using a FerroOrange probe (DOJINDO, #F374, Japan). After treatment according to the experimental protocol, the culture medium was discarded, HT22 cells were washed three times with PBS solution, and the FerroOrange working solution with a final concentration of 1 μmol/L was diluted with DMEM and processed for 30 minutes at 37°C in a 5% CO_2 incubator, nuclei were stained by adding 5 ul of Hoechst 33342 (Beyotime, # C1025, China) staining solution, incubated for 5 min at room temperature and protected from light. Finally, the stained cells were observed using a fluorescence microscope.

2.6. Iron measurement

Intracellular ferrous iron levels were assessed using an iron assay kit (Elabscience, #E-BC-K881-M, China). Prior to the experiment, the standard protectant was mixed with the buffer as required. After the indicated treatments, HT22 cells were harvested to lysed cells by adding 0.2 mL of buffer per 1×10^6 cells, centrifuged at 15,000×g for 10 min, and the supernatant was taken for ferrous iron measurement assay. Experimental procedures strictly followed the manufacturer's instructions.

2.7. MDA measurement

Intracellular MDA concentration was assessed using a Lipid Peroxidation MDA Assay Kit (Beyotime, #S0131, China). After the indicated treatments, HT22 cells were harvested and lysed in RIPA lysate. Cell lysates were centrifuged at 15,000 rpm for 10 min, and the supernatant was collected for subsequent experiments. The MDA measurement procedure strictly followed the manufacturer's instructions.

2.8. ROS level detection

Dilute DCFH-DA (Beyotime, #S0033S, China). with serum-free culture medium according to 1:1,000 to give a final concentration of 10 μmol/L. An appropriate amount was added to the well plate, covered with the sample, and incubated for 20 min at 37°C in a cell culture incubator. Using a flow cytometric analyzer, set the excitation wavelength of 488 nm and the emission wavelength of 525 nm to detect the intensity of fluorescence after stimulation. All experimental operations were performed in strict accordance with the reagent instructions.

2.9. Annexin V-FITC PI apoptosis

HT22 cell death was assessed using the Annexin V - FITC PI Apoptosis Kit (Lianke, #AT101, China), which has strict instructions for use. According to the experimental design, digested with matching trypsin for 5-10 minutes at room temperature after intervention, added pre-cooled PBS, mixed by gentle blowing, collected into tubes and centrifuged, resuspended by adding 500 μL of Apoptosis Positive Control Reagent, incubated on ice for 30 minutes, resuspended by adding an appropriate amount of pre-cooled 1× Binding Solution, and added the same number of untreated live cells to mix with it. Added 1× Binding Solution to reach a total volume of 1.5 mL, the suspension was divided equally into three tubes: a blank control tube, a PI single-stained tube, and an Annexin V-FITC single-stained tube. Annexin V-FITC (5 μL) or PI (10 μL) was added to the single-stained tubes, while both Annexin V-FITC (5 μL) and PI (10 μL) were added to the tubes containing samples to be examined. Incubate the tubes for 5 min at room temperature and avoiding light, and then turn on the flow cytometer, and detect the samples through the FITC (Ex = 488 nm, Em = 530 nm) and PI (Ex = 535 nm, Em = 615 nm) channels.

2.10. Immunofluorescence

Cell culture plates used for immunofluorescence experiments were previously coated with 1% gelatin aqueous solution. After cell intervention, 4% paraformaldehyde was added to fix it for 15 min, 0.3% Triton X-100 was added, treated for 15 min, blocked with 5% goat serum, and incubated for 1 hour at 37°C. Finally, the samples were incubated with the primary antibody against microtubule-associated protein 2 (MAP2) (Abcam, #ab183830, dilution 1:500) at 4°C overnight. The next day, samples were washed three times with PBST and incubated with anti-rabbit IgG (Invitrogen, #A21207, USA, Alexa Fluor 594, dilution 1:100) secondary antibody for 60 min at room temperature. The nuclei were then stained with DAPI (Beyotime, #C1005, China) solution for 5 minutes. Images were acquired using an orthogonal fluorescence microscope.

2.11. Western blot assays

Total cellular proteins were extracted using SDS lysis buffer supplemented with protease and phosphatase inhibitors, followed by protein electrophoresis. ACSL4 antibody (Santa Cruz Biotechnology, #sc-365230, diluted at 1:100), postsynaptic density protein 95 (PSD95) antibody (Invitrogen, #MA1-046, diluted at 1:500), FNDC5 antibody (Abcam, #ab174833, diluted at 1:1,000), β-actin antibody (Abcam, #ab115777, diluted at 1:1,000), were all shaken overnight and incubated. Next day, the samples were washed 5 times with PBST and incubated with goat anti-mouse HRP coupled secondary antibody (Proteintech, #20000838, dilution ratio 1:10,000) or goat anti-rabbit HRP coupled secondary antibody (zsbio, #ZB-2301, dilution ratio 1:5,000) for 1 hour at room temperature.

2.12. Statistical analysis

Data were presented as mean ± standard deviation (mean ± SD). All data were assessed for normality using appropriate statistical tests. Unpaired two-tailed t tests were used for comparing two independent groups, and one-way ANOVA was used for multiple group comparisons. Differences were considered statistically significant at *($P < 0.05$), **($P < 0.01$), and ***($P < 0.001$).

3. Results

3.1. High-glucose microenvironment induced neurotoxicity in HT22 cells

To investigate the effect of high glucose on HT22 cell viability, we treated cells with glucose concentrations of 25 mM (control group), 50 mM, and 75 mM (high glucose groups). Cell viability was assessed at 12, 24, 36, and 48 hours. High glucose treatments (50 mM and 75 mM) significantly inhibited HT22 cell proliferation and reduced cell viability at 36 hours (Figure 1A). Flow cytometry analysis revealed an apoptosis rate of 16.88% in HT22 cells at 36 hours with 75 mM glucose treatment, compared to 5.03% in the control group (Figure 1B). MAP2 immunofluorescent staining showed that 75

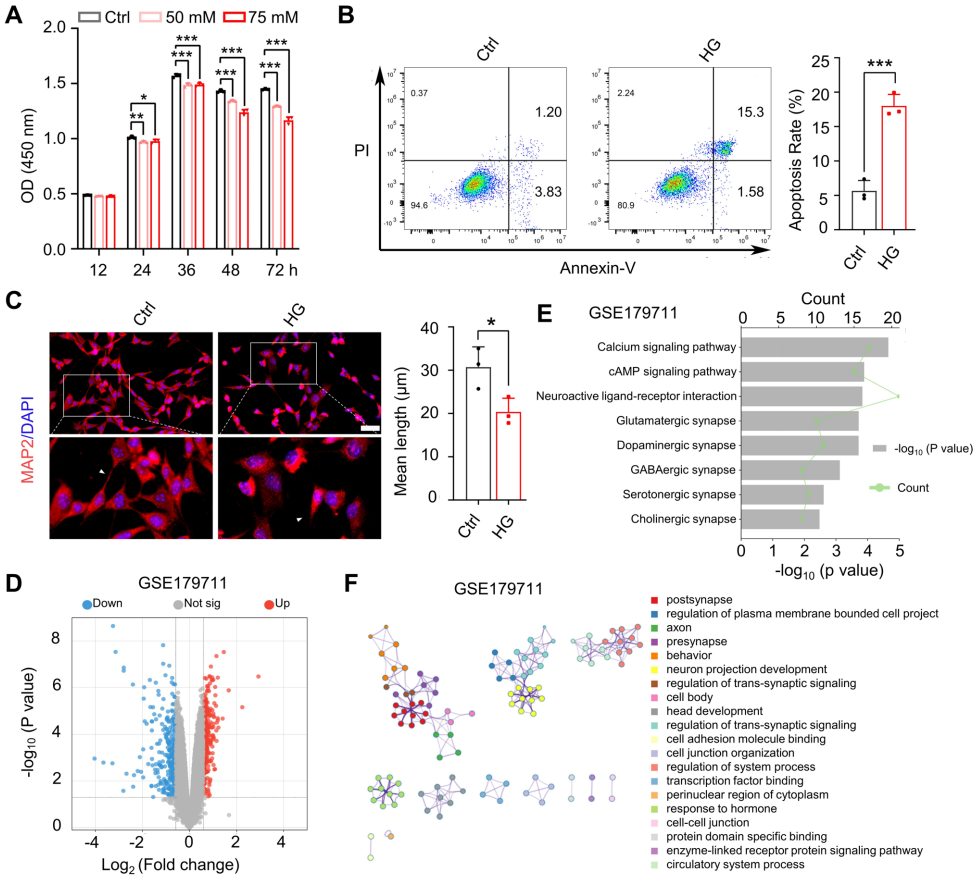

Figure 1. High-glucose microenvironment induced neurotoxicity in HT22 cells. (**A**) Cellular viability of HT22 cells was assessed at 12, 24, 36, 48, 72 hour after interventions with 25mM, 50mM, 75mM glucose . (**B**) Apoptosis rate analysis of HT22 cells was conducted using flow cytometry after high glucose (HG) interventions (**C**) Representative images of immunofluorescence staining of MAP2 (red) and DAPI (blue) were obtained after 36 hours of exposure to 75 mM high glucose. Scale bar = 50 μm. The mean neurite length, as indicated by MAP2 staining, was quantified. (**D**) Volcano plot displaying differentially expressed genes in the cerebral cortex of control mice and mice with impaired glucose tolerance in dataset GSE179711; (**E**) Analysis of the KEGG signaling pathway differential expression genes; (**F**) Analysis of the GO signaling pathway differential expression genes. Each experiment was conducted in triplicate. Statistical analyses were performed including unpaired Student's *t*-tests and one-way ANOVA. *($P < 0.05$), **($P < 0.01$), and ***($P < 0.001$).

mM glucose treatment for 36 hours reduced the length of neurite in HT22 cells (Figure 1C). Additionally, we analyzed RNA sequencing data from the cerebral cortex of mice with impaired glucose tolerance using the GSE179711 dataset (*20*) from the GEO database. Differential gene screening was performed with a fold change cutoff of 1.5 (Figure 1D). KEGG (Figure 1E) and GO pathway enrichment analyses (Figure 1F) indicated that the differential genes were primarily involved in the regulation of neural synapses and behavioral performance. These results are consistent with our findings that high glucose affects synaptic function and exerts neurotoxic effects.

3.2. High glucose triggers ferroptosis in HT22 cells

Based on the latest research, high glucose induces ferroptosis in mouse brain neurons (*21*). To investigate whether high glucose-induced neurotoxicity in HT22 cells is mediated by ferroptosis, we assessed intracellular Fe^{2+} and MDA levels at various time points following 75 mM high glucose intervention. We found a significant increase in ferrous ion levels at 36 hours (Figure 2A). Correspondingly, MDA levels increased progressively, peaking at 36 hours (Figure 2B). The occurrence of ferroptosis was further supported by a significant rise in ROS levels at 36 hours (Figure 2C). These results suggest that 75 mM high glucose intervention for 36 hours may induce ferroptosis in HT22 cells.

To further investigate high glucose-induced neurodegeneration in HT22 cells via ferroptosis, we selected Fer-1, a ferroptosis inhibitor known to effectively counter the ferroptosis cascade by interfering with lipid peroxidation and reducing oxidative stress. We treated high glucose-cultured HT22 cells with 1 μM Fer-1 (*22*) and observed that Fer-1 treatment significantly reduced intracellular MDA levels (Figure 2D) and decreased the accumulation of intracellular ferrous ions (Figure 2E). Additionally, Fer-1 treatment notably suppressed the expression of the ferroptosis marker protein ACSL4 induced by high glucose (Figure 2F). Using CCK8 assays, we found that Fer-1 treatment increased the viability of high glucose-treated cells (Figure 2G) and elevated the protein expression

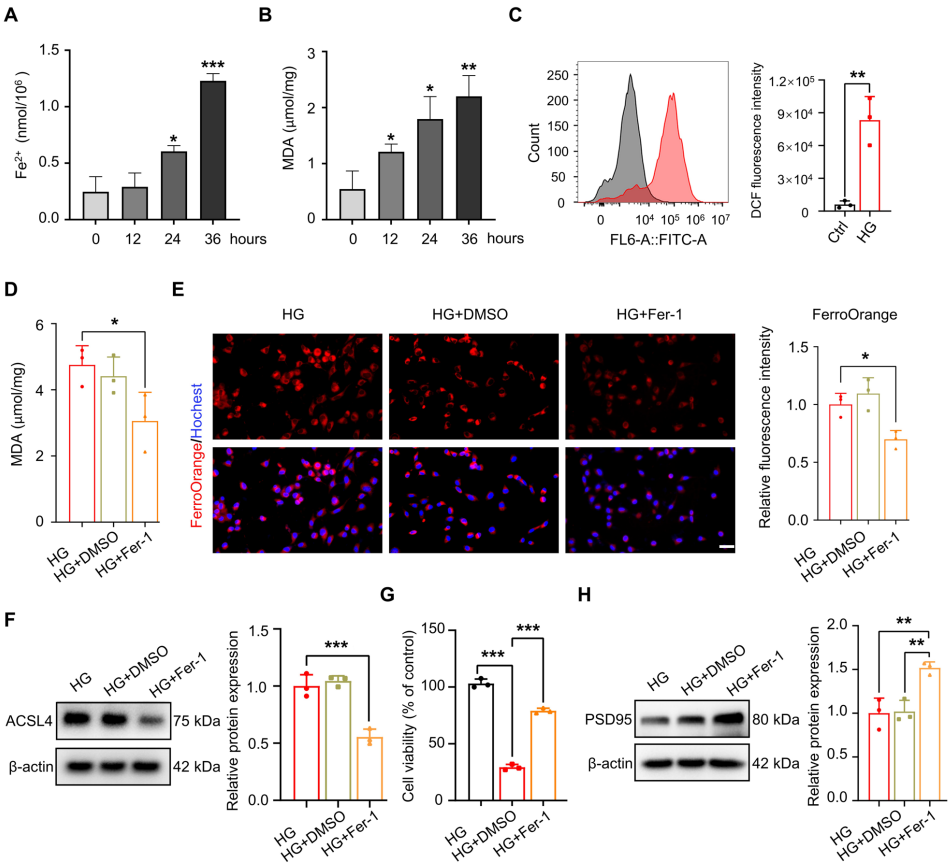

Figure 2. High glucose triggers ferroptosis in HT22 cells. Assessment of intracellular ferrous ion levels in HT22 cells following 75 mM glucose treatment at various time points (n = 3). (**B**) Assessment of MDA levels in HT22 cells following 75 mM glucose treatment at various time points (n = 3). (**C**) Measurement of ROS levels in HT22 cells after 36 hours of 75 mM glucose treatment using flow cytometry (n = 3). (**D**) Assessment of intracellular MDA levels in HT22 cells under high glucose conditions following treatment with iron death inhibitor Fer-1 (n = 3). (**E**) Intracellular ferrous ion levels in HT22 cells under high glucose conditions following treatment with Fer-1. Intracellular ferrous ions (FerroOrange, red) and nuclei (Hoechst, blue) was performed. Scale bar = 50 μm. (**F**) ACSL4 protein levels in HT22 cells under high glucose conditions following treatment with Fer-1. (**G**) Assessment of cellular activity in HT22 cells under high glucose conditions using CCK8 following treatment with Fer-1. (**H**) PSD95 protein levels in HT22 cells under high glucose conditions following treatment with Fer-1. Data are expressed as mean ± SD, each experiment was conducted in triplicate. Statistical analyses were performed including unpaired Student's t-tests. *($P < 0.05$), **($P < 0.01$), and ***($P < 0.001$).

of the synaptic marker PSD95 (Figure 2H). These results indicate that Fer-1 inhibit high glucose-induced ferroptosis and neurotoxicity, highlighting ferroptosis as a critical mechanism underlying high glucose-induced cytotoxicity in HT22 cells.

3.3. Exogenous irisin ameliorated high glucose-induced neurotoxicity and ferroptosis

Studies have reported that irisin can effectively improve insulin resistance and regulate glucose homeostasis (*23*), highlighting its positive role in ameliorating hyperglycaemic toxicity. However, whether irisin can exert neuroprotective effects by mitigating hyperglycaemia-induced ferroptosis remains unclear. Therefore, we explored the effects of irisin on HT22 cells in a hyperglycaemic environment. We first determined the effective concentration and safe dosage of irisin. Figure 3A illustrates a decline in cell activity in the high glucose environment, while no significant changes were noted in the mannitol osmolality control group. Notably, treatment with irisin from 0.1 to 10 nM significantly enhanced cell activity under high glucose conditions, with the most pronounced therapeutic effect observed at 5 nM irisin ($P < 0.05$). Therefore, 5 nM irisin was chosen for subsequent experiments (Figure 3A).

To validate the effect of irisin on HT22 cells in a high glucose environment, we examined cell activity and neurite length. We found that irisin significantly reduced the cell apoptosis rate (Figure 3B), increased neurite length (Figure 3C), and elevated PSD95 protein expression (Figure 3D), indicating that irisin exerts neuroprotective effects on HT22 cells under high glucose conditions. Subsequently, we investigated whether irisin could alleviate high glucose-induced ferroptosis in HT22 cells. We observed that irisin significantly decreased MDA levels (Figure 3E), intracellular ROS levels (Figure 3F), and intracellular ferrous ion levels (Figure 3G-H). In conclusion, irisin exerts neuroprotective effects in a high glucose environment by effectively inhibiting high glucose-induced intracellular iron overload, oxidative stress, and ferroptosis.

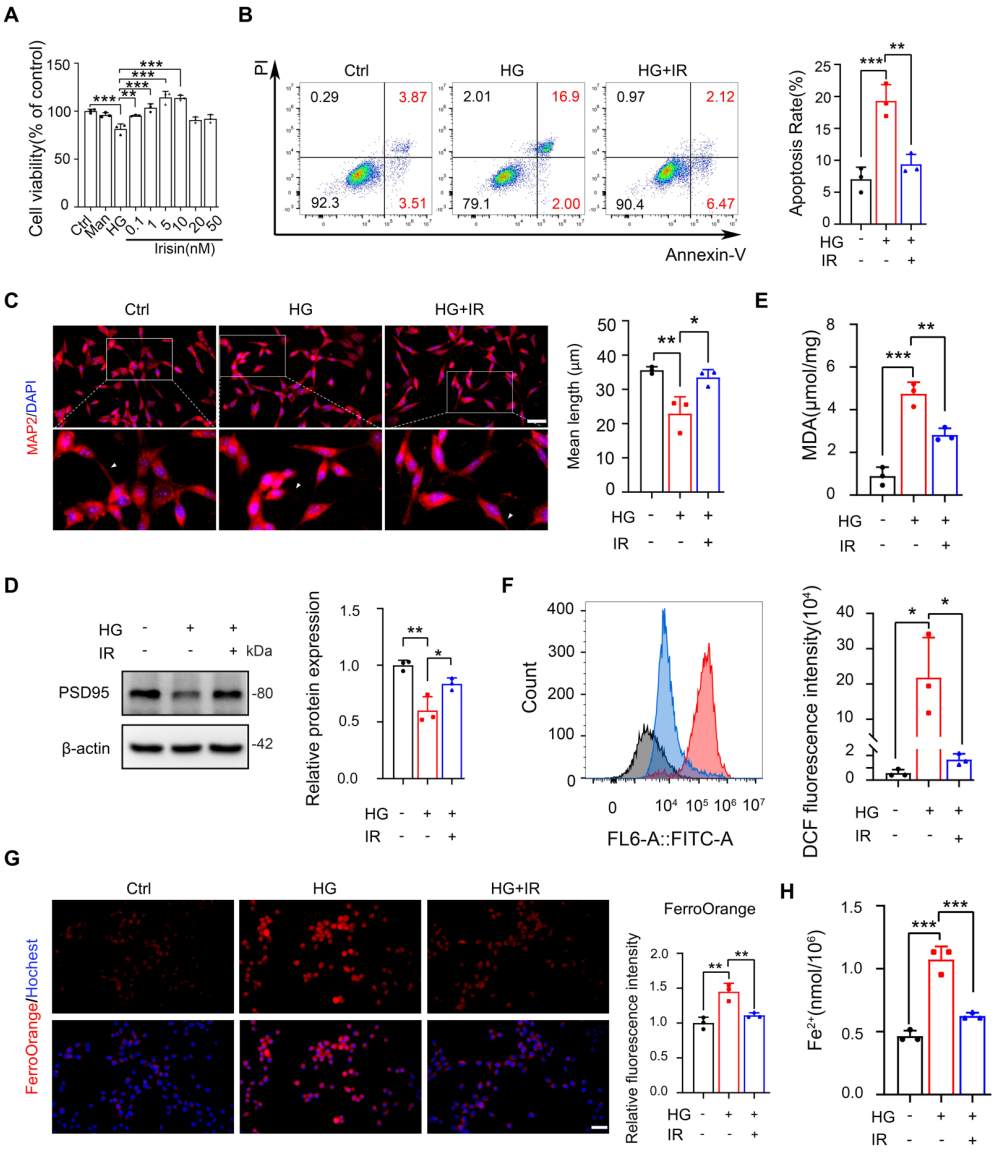

Figure 3. Exogenous irisin ameliorated high glucose-induced neurotoxicity and ferroptosis. (**A**) Assessment of cellular activity in HT22 cells treated with varying concentrations of irisin under high glucose conditions, using 50 nM mannitol as an osmotic control. (**B**) Assessment of apoptosis rate in HT22 cells treated with 5 nM irisin under high glucose conditions by flow cytometry. (**C**) Representative images of immunofluorescence staining of MAP2 (red) and DAPI (blue). Scale bar = 50 μm. The mean neurite length, as indicated by MAP2 staining, was quantified. (**D**) Protein levels of PSD95 in HT22 cells treated with 5 nM irisin under high glucose conditions. (**E**) Quantitative intracellular MDA levels in HT22 cells after treated with 5 nM irisin under high glucose conditions. (**F**) Flow cytometry detection of intracellular ROS levels in HT22 cells after treated with 5 nM irisin under high glucose conditions. (**G**) Intracellular ferrous fluorescence intensity of HT22 cells after treated with 5 nM irisin under high glucose conditions. Intracellular ferrous ions (FerroOrange, red) and nuclei (Hoechst, blue) was performed to count the average fluorescence intensity. Scale bar = 50 μm. (H) Quantitative levels of intracellular ferrous iron in HT22 cells after treated with 5 nM irisin under high glucose conditions. Each experiment was conducted in triplicate, data are expressed as mean ± SD. Statistical analyses were performed including unpaired Student's *t*-tests and one-way ANOVA. *($P < 0.05$), ** ($P < 0.01$), and ***($P < 0.001$).

3.4. FNDC5 overexpression mitigated high glucose-induced neurotoxicity and ferroptosis

Irisin is derived from the FNDC5 protein through proteolytic cleavage of its extracellular fragment and is subsequently secreted into the peripheral circulation. Our findings demonstrated that exogenous irisin exerts a neuroprotective effect on HT22 cells in a high glucose environment. This prompted us to investigate whether the expression of endogenous FNDC5 could have a similar impact. We first examined the protein expression of FNDC5 in HT22 cells under high glucose conditions and found that high glucose treatment inhibited FNDC5 expression compared to the control (Figure 4A). Based on this observation, we overexpressed FNDC5 in HT22 cells using plasmid transfection (Supplementary Figures S1. A-C, *https://www.biosciencetrends.com/action/getSupplementalData.php?ID=216*). Flow cytometry analysis revealed that FNDC5 overexpression decreased the apoptosis rate of HT22 cells in a high glucose environment (Figure 4B), improved the average length of neurite (Figure 4C), and increased the protein expression

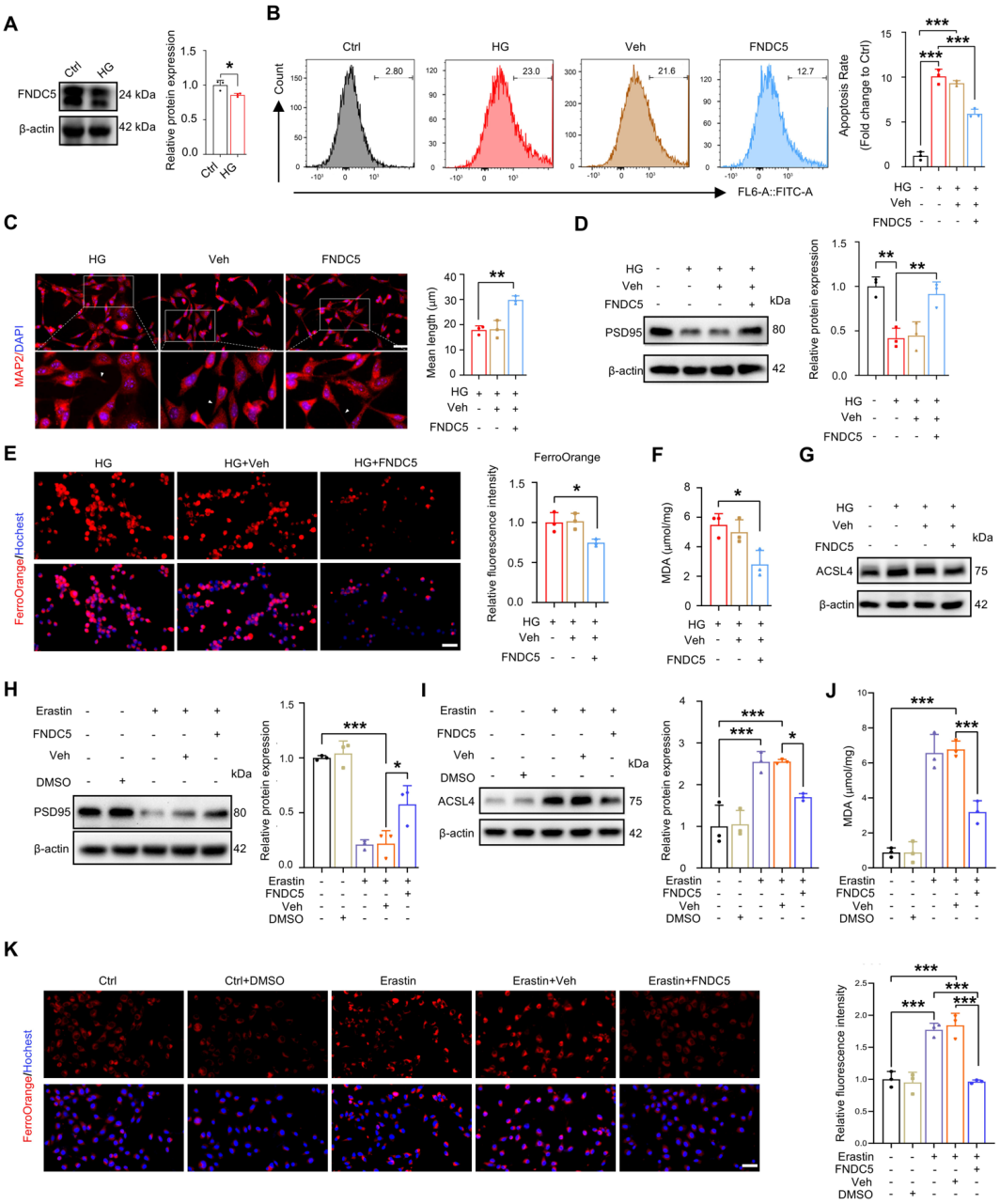

Figure 4. FNDC5 overexpression ameliorated high glucose-induced neurotoxicity and ferroptosis. (**A**) Endogenous FNDC5 protein expression levels in HT22 cells under high glucose. (**B**) Apoptosis rate in HT22 cells under high glucose conditions following FNDC5 overexpression, as measured by flow cytometry. (**C**) Representative images of immunofluorescence staining of MAP2 (red) and DAPI (blue). Scale bar = 50 μm. The mean neurite length, as indicated by MAP2 staining, was quantified. (**D**) Protein levels of PSD95 in HT22 cells under high glucose conditions following FNDC5 overexpression. (**E**) Intracellular ferrous fluorescence intensity of HT22 cells under high glucose conditions following FNDC5 overexpression. Intracellular ferrous ions (FerroOrange, red) and nuclei (Hoechst, blue) was performed to count the average fluorescence intensity. Scale bar 50 = μm. (**F**) Quantitative intracellular MDA levels. (**G**) Intracellular ACSL4 protein expression levels. (**H**) Intracellular PSD95 protein expression levels in erastin-treated HT22 cells with FNDC5 overexpression. (**I**) Intracellular ACSL4 protein expression levels. (**J**) Intracellular MDA levels. (**K**) Intracellular ferrous fluorescence intensity. Each experiment was conducted in triplicate, data are expressed as mean ± SD. Statistical analyses were performed including unpaired Student's *t*-tests and one-way ANOVA with Tukey's post hoc tests. *($P < 0.05$), **($P < 0.01$), and ***($P < 0.001$).

of PSD95 (Figure 4D).

In addition, we observed that overexpression of FNDC5 effectively reduced the intracellular ferrous ions (Figure 4E), MDA level (Figure 4F), and protein expression of ACSL4 (Figure 4G) in HT22 cells under high glucose conditions. These results suggest that overexpression of FNDC5 attenuates high glucose-induced neurotoxicity and ferroptosis. To further validate the effect of FNDC5 on ferroptosis, we tested the impact of FNDC5 overexpression using the ferroptosis inducer Erastin, which promotes ferroptosis through multiple mechanisms (*24*). We treated cells with 0.5 μM Erastin to induce ferroptosis and found that Erastin treatment inhibited the protein expression of PSD95 and increased

the protein expression of ACSL4, a marker of ferroptosis, in HT22 cells compared to controls. Overexpression of FNDC5 effectively increased PSD95 protein expression and decreased ACSL4 protein levels (Figure 4H-I). Additionally, we observed that Erastin-induced MDA levels and ferrous ion accumulation were alleviated by FNDC5 overexpression (Figure 4J-K). Taken together, these findings suggest that overexpression of FNDC5 in a high glucose environment attenuates neurotoxicity through the inhibition of ferroptosis.

3.5. Exogenous irisin attenuates high glucose-induced neurotoxicity under conditions of reduced FNDC5 expression

Due to the decreased expression of FNDC5 in a high glucose environment, leading to reduced endogenous irisin production, we aimed to investigate whether exogenous irisin could exert neuroprotective effects when FNDC5 expression is significantly reduced. We further knocked down FNDC5 expression in HT22 cells under high glucose conditions (Supplementary Figure S1. E-F, *https://www.biosciencetrends.com/action/getSupplementalData.php?ID=216*) and then treated the cells with exogenous irisin. The results showed that irisin treatment effectively reduced the apoptosis rate in the FNDC5 knockdown group under high glucose conditions (Figure 5A), prolonged the average neurite length (Figure 5B), and increased the PSD95 protein expression level

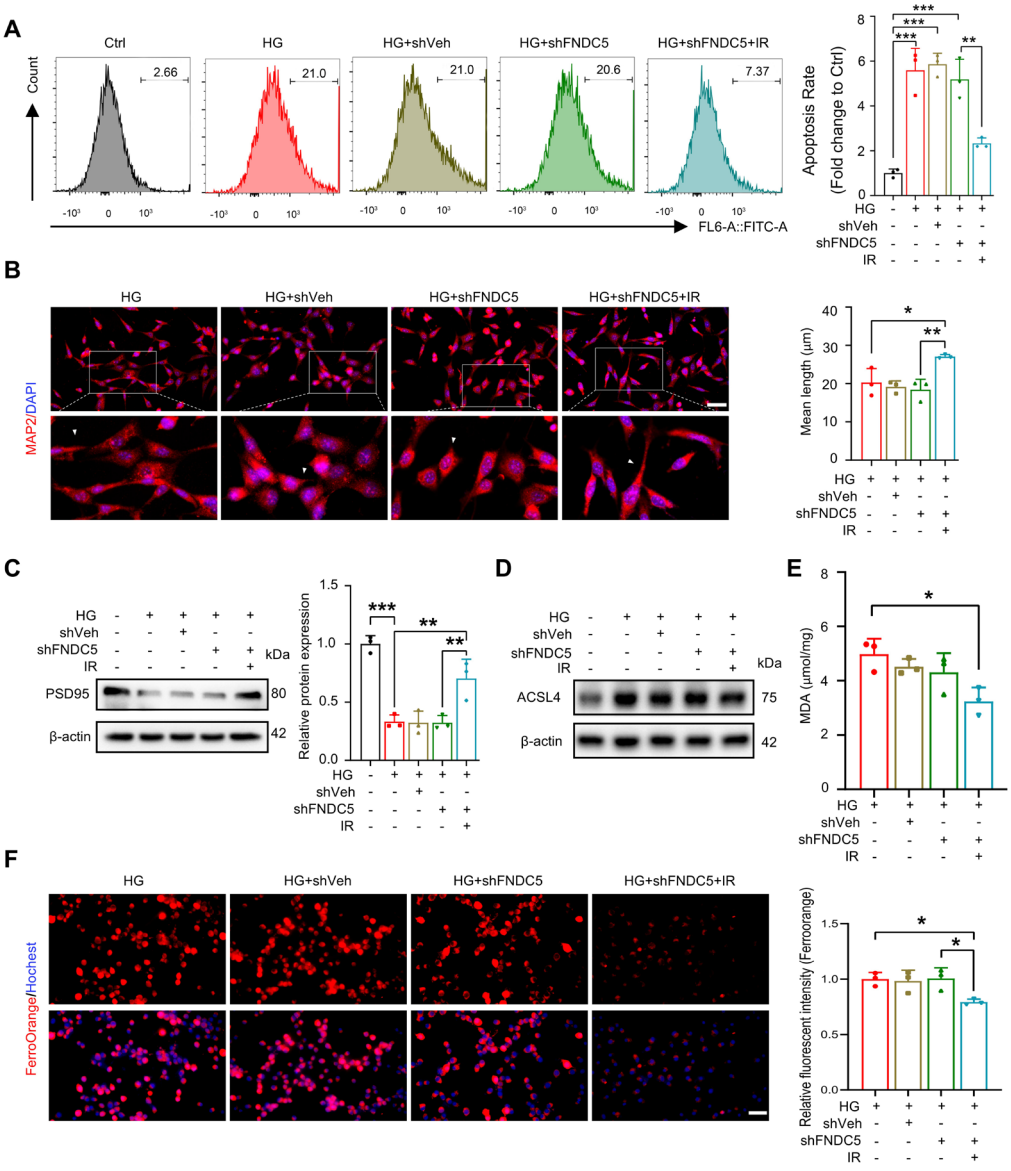

Figure 5. Exogenous Irisin administration after FNDC5 knockdown ameliorated high glucose-induced neurotoxicity. (A) Apoptosis detection by flow cytometry in HT22 cells with FNDC5 knockdown following irisin intervention. (**B**) Representative images of immunofluorescence staining of MAP2 (red) and DAPI (blue). Scale bar = 50 μm. The mean neurite length, as indicated by MAP2 staining, was quantified. (**C**) Protein levels of PSD95. (**D**) Intracellular ACSL4 protein expression levels. (**E**) Quantitative intracellular MDA levels. (**F**) Intracellular ferrous fluorescence intensity of HT22 cells with FNDC5 knockdown following irisin intervention. Ferrous ions (FerroOrange, red) and nuclei (Hoechst, blue). Scale bar = 50 μm. Each experiment was conducted in triplicate, data are expressed as mean ± SD. Statistical analyses were performed including unpaired Student's *t*-tests and one-way ANOVA with Tukey's post hoc tests. *($P < 0.05$), **($P < 0.01$), and ***($P < 0.001$).

(Figure 5C). Similarly, irisin treatment also inhibited ferroptosis-related markers in FNDC5 knockdown HT22 cells under high glucose conditions, including ACSL4 expression (Figure 5D), MDA levels (Figure 5E), and intracellular ferrous ion levels (Figure 5F). In conclusion, with endogenous FNDC5 knockdown, irisin effectively alleviated high glucose-induced neurotoxicity and ferroptosis in HT22 cells. These results further underscore the effectiveness of irisin in mitigating high glucose-induced neurotoxicity.

4. Discussion

With the aging population, diabetes has emerged as a major global health concern, particularly in the elderly. Diabetic neuropathy represents a critical complication of diabetes, underscoring the importance of elucidating the mechanisms linking hyperglycemia to nerve damage and identifying potential therapeutic interventions.

In this study, we demonstrated that high glucose exerts neurotoxic effects on HT22 cells, as evidenced by reduced cellular viability, increased apoptosis, shortened neurite length, and decreased expression of the synaptic marker protein PSD95. Furthermore, we observed activation of the ferroptosis pathway in high-glucose-treated HT22 cells, characterized by iron overload, oxidative stress, lipid peroxidation, and elevated expression of the ferroptosis marker ACSL4. Notably, irisin treatment effectively suppressed high-glucose-induced neurotoxicity and ferroptosis in these cells. Additionally, high glucose reduced the expression of FNDC5, the precursor protein of irisin. Overexpression of FNDC5 increased endogenous irisin levels, resulting in neuroprotection and inhibition of ferroptosis. To further explore this mechanism, we knocked down FNDC5 expression and treated the cells with exogenous irisin. Remarkably, exogenous irisin supplementation attenuated neurotoxicity and inhibited ferroptosis, even in the context of reduced endogenous FNDC5 expression. In conclusion, our findings indicate that FNDC5/irisin mitigates high-glucose-induced neurotoxicity by inhibiting ferroptosis in HT22 cells, offering new insights and potential therapeutic strategies for diabetic neuropathy.

The expression of ferroptosis-related markers, including glutathione peroxidase 4 (GPX4) and the cystine/glutamate antiporter (SLC7A11), was markedly downregulated in a high-glucose environment. In contrast, ferritin levels and lipid peroxidation were significantly elevated (*25,26*), indicating that ferroptosis is a key mechanism underlying high-glucose-induced cytotoxicity. Our experimental findings demonstrated that FNDC5/Irisin significantly attenuated lipid peroxidation and intracellular iron accumulation, thereby inhibiting ferroptosis. In line with previous studies, FNDC5/Irisin was also shown to suppress the expression of inducible nitric oxide synthase (iNOS) and NADPH oxidase 2 (NOX2), reducing ROS production under high-glucose conditions (*27*). Moreover, Irisin reduced ferroptosis by downregulating elevated levels of superoxide dismutase (SOD), glutathione peroxidase 1 (GPX-1), catalase (CAT), and Nrf2, thereby mitigating oxidative stress induced by high glucose (*28*). These findings suggest that FNDC5/Irisin may represent a promising therapeutic target for diabetes-associated neuropathy and other ferroptosis-related pathologies. Further research is warranted to elucidate the precise regulatory mechanisms of FNDC5/Irisin in ferroptosis and explore its potential clinical applications.

In addition, we observed a reduction in FNDC5 expression in HT22 cells under high-glucose conditions. Previous studies have shown that FNDC5 expression in subcutaneous adipose tissue of type II diabetic patients is reduced by 40–45%, while circulating irisin levels decrease by 40%. Furthermore, circulating irisin levels are negatively correlated with fasting blood glucose (*27,29,30*) and diabetic complications (*29,31*). Similarly, an in vitro study demonstrated that high glucose suppresses FNDC5 mRNA and protein expression in a concentration-dependent manner (*32*); however, the underlying mechanism for this reduction remains unclear. In a related study, decreased expression of cystathionine γ-lyase in high-glucose mice led to H2S deficiency, which triggers excessive oxidative stress and impairs PGC-1α expression (*18*). As FNDC5 expression in neurons is heavily dependent on PGC-1α activity (*33*), it is plausible that downregulation of PGC-1α in high-glucose environments contributes to the reduced expression of FNDC5/irisin. Additionally, inflammatory factors and oxidative stress have been shown to influence FNDC5 expression; for example, IL-1β and TNFα reduce FNDC5 protein synthesis and lower irisin levels (*31,34*). Previous research suggests that high glucose inhibits the ERK/MAPK signaling pathway (*35*), which is known to positively regulate PGC-1α/FNDC5/irisin expression during neuronal differentiation (*36*). Thus, downregulation of the ERK/MAPK pathway may represent an additional mechanism contributing to the reduction in FNDC5/irisin expression.

Given the reduction in FNDC5/irisin expression under high-glucose conditions, and its established neuroprotective effects, restoring FNDC5/irisin levels is crucial for mitigating high-glucose-induced neurological damage. Our findings indicate that exogenous irisin supplementation, despite reduced FNDC5 expression, attenuated high-glucose-induced neurotoxicity and ferroptosis. Previous studies have shown that adenovirus-mediated delivery of FNDC5 to the liver increases circulating irisin levels, which, in turn, induces the expression of neuroprotective factors in the hippocampus (*33*). Thus, therapeutic strategies centered on injectable peptides targeting FNDC5/irisin may represent a promising approach to mitigate diabetic neurotoxicity. However, further studies are required to evaluate the

clinical efficacy of FNDC5/irisin in preventing diabetic neurotoxicity and cognitive impairment. While this study focuses on the role of FNDC5/irisin in neuronal cells, the significance of myogenic FNDC5/irisin should not be underestimated. FNDC5/irisin, a myokine, is highly expressed in skeletal muscle, and approximately 70% of circulating irisin in mice originates from muscle tissue (*18*). Its secretion is significantly elevated in response to exercise (*37*), and muscle-derived irisin can cross the blood-brain barrier, enabling it to influence the central nervous system. Moreover, exercise has been shown to upregulate FNDC5 expression in the hippocampus, subsequently increasing the levels of brain-derived neurotrophic factor (BDNF) and providing neuroprotection (*33*). These observations suggest that exercise-induced upregulation of FNDC5/irisin could represent a promising intervention to mitigate the cognitive dysfunction associated with diabetes mellitus

Furthermore, although our study provides strong evidence that FNDC5/Irisin alleviates high glucose-induced neurotoxicity in HT22 cells, several limitations remain. First, our study was conducted primarily at the cellular level and lacked validation in animal models. Second, it is unclear whether FNDC5/Irisin exerts consistent effects across different types of neuronal cells, necessitating further investigation. Additionally, other potential mechanisms, such as the interaction of FNDC5/Irisin with other signaling pathways, warrant further exploration.

In conclusion, our findings highlight the role of FNDC5/irisin in alleviating high glucose-induced neurotoxicity and ferroptosis, presenting a novel target for the treatment of diabetes-associated neurodegenerative diseases and providing a foundation for future clinical studies.

Acknowledgements

We express our gratitude to the Chongqing Key Laboratory of Translational Medicine for Cognitive Development and Learning and Memory Disorders, Institute of Paediatrics, Affiliated Children's Hospital of Chongqing Medical University for generously providing the HT22 mouse hippocampal cells. We extend our gratitude to the research platform of the Second Affiliated Hospital of Chongqing Medical University for their invaluable support and assistance. We acknowledge the Gene Expression Omnibus (GEO) for providing public access to its data.

Funding: This work was funded by the National Natural Science Foundation of China (Grant No.82371427, Grant No.82401656), Natural Science Foundation of Chongqing, China (CSTB2023NSCQBHX0018, CSTB2023NSCQ-MSX0323), Kuanren Talents Program of the Second Affiliated Hospital of Chongqing Medical University (Grant No. kryc-lj-2105) and Postgraduate Research and Innovation Project of Chongqing Province (Grant No. CYB240199).

Conflict of Interest: The authors have no conflicts of interest to disclose.

References

1. GBD 2021 Diabetes Collaborators. Global, regional, and national burden of diabetes from 1990 to 2021, with projections of prevalence to 2050: a systematic analysis for the Global Burden of Disease Study 2021. Lancet. 2023; 402:203-234.
2. Stumvoll M, Goldstein BJ, van Haeften TW. Type 2 diabetes: principles of pathogenesis and therapy. Lancet. 2005; 365:1333-46.
3. Taylor R. Type 2 diabetes: etiology and reversibility. Diabetes Care. 2013; 36:1047-55.
4. Xu L, Li Y, Dai Y, Peng J. Natural products for the treatment of type 2 diabetes mellitus: Pharmacology and mechanisms. Pharmacol Res. 2018; 130:451-465.
5. You Y, Liu Z, Chen Y, Xu Y, Qin J, Guo S, Huang J, Tao J. The prevalence of mild cognitive impairment in type 2 diabetes mellitus patients: a systematic review and meta-analysis. Acta Diabetol. 2021; 58:671-685.
6. Xue M, Xu W, Ou YN, Cao XP, Tan MS, Tan L, Yu JT. Diabetes mellitus and risks of cognitive impairment and dementia: A systematic review and meta-analysis of 144 prospective studies. Ageing Res Rev. 2019; 55:100944.
7. Yang Q, Zhou L, Liu C, Liu D, Zhang Y, Li C, Shang Y, Wei X, Li C, Wang J. Brain iron deposition in type 2 diabetes mellitus with and without mild cognitive impairment-an in vivo susceptibility mapping study. Brain Imaging Behav. 2018; 12:1479-1487.
8. An JR, Su JN, Sun GY, Wang QF, Fan YD, Jiang N, Yang YF, Shi Y. Liraglutide Alleviates Cognitive Deficit in db/db Mice: Involvement in Oxidative Stress, Iron Overload, and Ferroptosis. Neurochem Res. 2022; 47:279-294.
9. Wang Z, Feng S, Li Q, Song Z, He J, Yang S, Yan C, Ling H. Dihydromyricetin alleviates hippocampal ferroptosis in type 2 diabetic cognitive impairment rats via inhibiting the JNK-inflammatory factor pathway. Neurosci Lett. 2023; 812:137404.
10. Xie Z, Wang X, Luo X, Yan J, Zhang J, Sun R, Luo A, Li S. Activated AMPK mitigates diabetes-related cognitive dysfunction by inhibiting hippocampal ferroptosis. Biochem Pharmacol. 2023; 207:115374.
11. Guo T, Yu Y, Yan W, Zhang M, Yi X, Liu N, Cui X, Wei X, Sun Y, Wang Z, Shang J, Cui W, Chen L. Erythropoietin ameliorates cognitive dysfunction in mice with type 2 diabetes mellitus via inhibiting iron overload and ferroptosis. Exp Neurol. 2023; 365:114414.
12. Dun SL, Lyu RM, Chen YH, Chang JK, Luo JJ, Dun NJ. Irisin-immunoreactivity in neural and non-neural cells of the rodent. Neuroscience. 2013; 240:155-62.
13. Piya MK, Harte AL, Sivakumar K, Tripathi G, Voyias PD, James S, Sabico S, Al-Daghri NM, Saravanan P, Barber TM, Kumar S, Vatish M, McTernan PG. The identification of irisin in human cerebrospinal fluid: influence of adiposity, metabolic markers, and gestational diabetes. Am J Physiol Endocrinol Metab. 2014; 306:E512-8.
14. Lourenco MV, Frozza RL, de Freitas GB, *et al*. Exercise-linked FNDC5/irisin rescues synaptic plasticity and memory defects in Alzheimer's models. Nat Med. 2019;

25:165-175.
15. Islam MR, Valaris S, Young MF, *et al*. Exercise hormone irisin is a critical regulator of cognitive function. Nat Metab. 2021; 3:1058-1070.
16. Wang J, Zhao YT, Zhang LX, Dubielecka PM, Qin G, Chin YE, Gower AC, Zhuang S, Liu PY, Zhao TC. Irisin deficiency exacerbates diet-induced insulin resistance and cardiac dysfunction in type II diabetes in mice. Am J Physiol Cell Physiol. 2023; 325:C1085-C1096.
17. Yano N, Zhang L, Wei D, Dubielecka PM, Wei L, Zhuang S, Zhu P, Qin G, Liu PY, Chin YE, Zhao TC. Irisin counteracts high glucose and fatty acid-induced cytotoxicity by preserving the AMPK-insulin receptor signaling axis in C2C12 myoblasts. Am J Physiol Endocrinol Metab. 2020; 318:E791-E805.
18. Boström P, Wu J, Jedrychowski MP, *et al*. A PGC1-α-dependent myokine that drives brown-fat-like development of white fat and thermogenesis. Nature. 2012; 481:463-8.
19. Wang J, Zhu Q, Wang Y, Peng J, Shao L, Li X. Irisin protects against sepsis-associated encephalopathy by suppressing ferroptosis via activation of the Nrf2/GPX4 signal axis. Free Radic Biol Med. 2022; 187:171-184.
20. Yoon G, Cho KA, Song J, Kim YK. Transcriptomic Analysis of High Fat Diet Fed Mouse Brain Cortex. Front Genet. 2019; 10:83.
21. Yu J, Zhang Y, Zhu Q, Ren Z, Wang M, Kong S, Lv H, Xu T, Xie Z, Meng H, Han J, Che H. A mechanism linking ferroptosis and ferritinophagy in melatonin-related improvement of diabetic brain injury. iScience. 2024; 27:109511.
22. Chen Y, He W, Wei H, Chang C, Yang L, Meng J, Long T, Xu Q, Zhang C. Srs11-92, a ferrostatin-1 analog, improves oxidative stress and neuroinflammation via Nrf2 signal following cerebral ischemia/reperfusion injury. CNS Neurosci Ther. 2023; 29:1667-1677.
23. Perakakis N, Triantafyllou GA, Fernández-Real JM, Huh JY, Park KH, Seufert J, Mantzoros CS. Physiology and role of irisin in glucose homeostasis. Nat Rev Endocrinol. 2017; 13:324-337.
24. Zhao Y, Li Y, Zhang R, Wang F, Wang T, Jiao Y. The Role of Erastin in Ferroptosis and Its Prospects in Cancer Therapy. Onco Targets Ther. 2020; 13:5429-5441
25. Feng S, Tang D, Wang Y, *et al*. The mechanism of ferroptosis and its related diseases. Mol Biomed. 2023; 4:33.
26. Miao R, Fang X, Zhang Y, Wei J, Zhang Y, Tian J. Iron metabolism and ferroptosis in type 2 diabetes mellitus and complications: mechanisms and therapeutic opportunities. Cell Death Dis. 2023; 14:186.
27. Lin C, Guo Y, Xia Y, Li C, Xu X, Qi T, Zhang F, Fan M, Hu G, Zhao H, Zhao H, Liu R, Gao E, Yan W, Tao L. FNDC5/Irisin attenuates diabetic cardiomyopathy in a type 2 diabetes mouse model by activation of integrin αV/β5-AKT signaling and reduction of oxidative/nitrosative stress. J Mol Cell Cardiol. 2021; 160:27-41.
28. Fu J, Li F, Tang Y, Cai L, Zeng C, Yang Y, Yang J. The Emerging Role of Irisin in Cardiovascular Diseases. J Am Heart Assoc. 2021; 10:e022453.
29. Kurdiova T, Balaz M, Vician M, *et al*. Effects of obesity, diabetes and exercise on Fndc5 gene expression and irisin release in human skeletal muscle and adipose tissue: in vivo and in vitro studies. J Physiol. 2014; 592:1091-107.
30. Moreno-Navarrete JM, Ortega F, Serrano M, Guerra E, Pardo G, Tinahones F, Ricart W, Fernández-Real JM. Irisin is expressed and produced by human muscle and adipose tissue in association with obesity and insulin resistance. J Clin Endocrinol Metab. 2013; 98:E769-78.
31. Parsanathan R, Jain SK. Hydrogen Sulfide Regulates Irisin and Glucose Metabolism in Myotubes and Muscle of HFD-Fed Diabetic Mice. Antioxidants (Basel). 2022; 11:1369.
32. Deng J, Zhang N, Chen F, Yang C, Ning H, Xiao C, Sun K, Liu Y, Yang M, Hu T, Zhang Z, Jiang W. Irisin ameliorates high glucose-induced cardiomyocytes injury via AMPK/mTOR signal pathway. Cell Biol Int. 2020; 44:2315-2325.
33. Wrann CD, White JP, Salogiannnis J, Laznik-Bogoslavski D, Wu J, Ma D, Lin JD, Greenberg ME, Spiegelman BM. Exercise induces hippocampal BDNF through a PGC-1α/FNDC5 pathway. Cell Metab. 2013; 18:649-59.
34. Matsuo Y, Gleitsmann K, Mangner N, Werner S, Fischer T, Bowen TS, Kricke A, Matsumoto Y, Kurabayashi M, Schuler G, Linke A, Adams V. Fibronectin type III domain containing 5 expression in skeletal muscle in chronic heart failure-relevance of inflammatory cytokines. J Cachexia Sarcopenia Muscle. 2015; 6:62-72.
35. Kumar P, Rao GN, Pal BB, Pal A. Hyperglycemia-induced oxidative stress induces apoptosis by inhibiting PI3-kinase/Akt and ERK1/2 MAPK mediated signaling pathway causing downregulation of 8-oxoG-DNA glycosylase levels in glial cells. Int J Biochem Cell Biol. 2014; 53:302-19.
36. Hosseini Farahabadi SS, Ghaedi K, Ghazvini Zadegan F, Karbalaie K, Rabiee F, Nematollahi M, Baharvand H, Nasr-Esfahani MH. ERK1/2 is a key regulator of Fndc5 and PGC1α expression during neural differentiation of mESCs. Neuroscience. 2015; 297:252-61.
37. Löffler D, Müller U, Scheuermann K, Friebe D, Gesing J, Bielitz J, Erbs S, Landgraf K, Wagner IV, Kiess W, Körner A. Serum irisin levels are regulated by acute strenuous exercise. J Clin Endocrinol Metab. 2015; 100:1289-99.

Received August 28, 2024; Revised October 8, 2024; Accepted October 14, 2024.

[§]These authors contributed equally to this work.
**Address correspondence to:*
Xiuqing Yao and Yaxi Luo, Department of Rehabilitation, The Second Affiliated Hospital of Chongqing Medical University, Chongqing, China.
E-mail: dryaoxq@cqmu.edu.cn (XY), luoyaxi@hospital.cqmu.edu.cn (YL)

Released online in J-STAGE as advance publication October 17, 2024.